

## FEATURED ARTICLE

# Development of a quantitative semi-mechanistic model of Alzheimer's disease based on the amyloid/tau/neurodegeneration framework (the Q-ATN model)

Norman A. Mazer<sup>1</sup>  | Carsten Hofmann<sup>1</sup> | Dominik Lott<sup>1</sup> | Ronald Gieschke<sup>1</sup> | Gregory Klein<sup>1</sup> | Frank Boess<sup>2</sup> | Hans Peter Grimm<sup>1</sup> | Geoffrey A. Kerchner<sup>1</sup> | Monika Baudler-Klein<sup>2</sup> | Janice Smith<sup>3</sup> | Rachelle S. Doody<sup>2,4</sup> | for the Alzheimer's Disease Neuroimaging Initiative

<sup>1</sup>Roche Pharma Research & Early Development, Roche Innovation Center, Basel, Switzerland

<sup>2</sup>F. Hoffmann-La Roche Ltd, Basel, Switzerland

<sup>3</sup>Roche Products Ltd, Welwyn Garden City, UK

<sup>4</sup>Genentech, Inc., South San Francisco, California, USA

## Correspondence

Norman A. Mazer, Roche Pharma Research and Early Development, Roche Innovation Center, Basel, Switzerland.

Email: [norman.mazer@roche.com](mailto:norman.mazer@roche.com)

Ronald Gieschke was an employee of F. Hoffmann-La Roche Ltd. at the time of this work; he is currently acting as a consultant for F. Hoffmann-La Roche.

Data used in preparation of this article were obtained from the Alzheimer's Disease Neuroimaging Initiative (ADNI) database ([adni.loni.usc.edu](http://adni.loni.usc.edu)). As such, the investigators within the ADNI contributed to the design and implementation of ADNI and/or provided data but did not participate in the analysis or writing of this report. A complete listing of ADNI investigators can be found at: [http://adni.loni.usc.edu/wp-content/uploads/how\\_to\\_apply/ADNI\\_Acknowledgement\\_List.pdf](http://adni.loni.usc.edu/wp-content/uploads/how_to_apply/ADNI_Acknowledgement_List.pdf)

## Abstract

**Introduction:** A quantitative model of Alzheimer's disease (AD) based on the amyloid/tau/neurodegeneration biomarker framework (Q-ATN model) was developed to sequentially link amyloid positron emission tomography (PET), tau PET, medial temporal cortical thickness, and clinical outcome (Clinical Dementia Rating – Sum of Boxes; CDR-SB).

**Methods:** Published data and biologically plausible mechanisms were used to construct, calibrate, and validate the model. Clinical trial simulations were performed for different anti-amyloid antibodies, including a 5-year simulation of subcutaneous gantenerumab treatment.

**Results:** The simulated time-course of biomarkers and CDR-SB was consistent with natural history studies and described the effects of several anti-amyloid antibodies observed in trials with positive and negative (or non-significant) outcomes. The 5-year simulation predicts that the beneficial effects of continued anti-amyloid treatment should increase markedly over time.

**Discussion:** The Q-ATN model offers a novel approach for linking amyloid PET to CDR-SB, and provides theoretical support for the potential clinical benefit of anti-amyloid therapy.

## KEYWORDS

aducanumab, amyloid, anti-amyloid therapies, bapineuzumab, biomarkers, Clinical Dementia Rating – Sum of Boxes, donanemab, gantenerumab, lecanemab, mathematical model, neurodegeneration, tau

This is an open access article under the terms of the [Creative Commons Attribution-NonCommercial](https://creativecommons.org/licenses/by-nc/4.0/) License, which permits use, distribution and reproduction in any medium, provided the original work is properly cited and is not used for commercial purposes.

© 2022 The Authors. *Alzheimer's & Dementia* published by Wiley Periodicals LLC on behalf of Alzheimer's Association.

### Highlights

- A semi-mechanistic model was developed to link amyloid/tau/neurodegeneration biomarkers to clinical outcome (Q-ATN model).
- The Q-ATN model describes the disease progression seen in natural history studies.
- Model simulations agree well with mean data from the aducanumab EMERGE study.
- A 5-year simulation of gantenerumab predicts greater benefit with longer treatment.

## 1 | BACKGROUND

With the recent US Food and Drug Administration (FDA) approval of aducanumab,<sup>1</sup> anti-amyloid therapy is now available for the treatment of early Alzheimer's disease (AD), and other anti-amyloid antibodies sharing similar pharmacological properties are on the horizon.<sup>2,3</sup> Although not without controversy,<sup>4</sup> the FDA's decision was based, in part, on a review of clinical trial data from a number of anti-amyloid antibodies, from which they concluded that a clear and consistent relationship exists between the extent of amyloid plaque removal and the magnitude of clinical benefit.<sup>1</sup>

Although it has long been hypothesized that amyloid plaque formation initiates a pathological cascade leading to symptomatic AD,<sup>5</sup> it is not self-evident that removing amyloid plaque after the start of the disease should result in clinical benefit. To address this fundamental question, a theoretical approach was taken to construct a semi-mechanistic mathematical model of the pathogenesis and treatment of AD based on the amyloid/tau/neurodegeneration (A/T/N) biomarker research framework proposed by Jack and colleagues.<sup>6,7</sup>

The quantitative A/T/N model (Q-ATN) uses literature data from natural history studies and anti-amyloid trials, and biologically plausible concepts to create a mathematical representation of the four sequential linkages between anti-amyloid treatment, amyloid positron emission tomography (PET) levels, tau PET levels, medial temporal cortical thickness (CT), and clinical outcome, that is, the Clinical Dementia Rating – Sum of Boxes (CDR-SB). These four linkages provide a set of quantitatively expressed hypotheses that can be tested by their ability to correctly describe the time-course of amyloid PET, tau PET, CT, and CDR-SB data reported in natural history studies<sup>8–10</sup> and during treatment with anti-amyloid antibodies.<sup>11–15</sup>

Following the initial validation of the Q-ATN model, A/T/N biomarkers and CDR-SB corresponding to a hypothetical 5-year study of gantenerumab treatment were simulated using the dosing regimen currently being investigated in the 27-month (116 weeks), Phase III GRADUATE trials (GRADUATE I, NCT03444870; GRADUATE II, NCT03443973).<sup>16</sup> The 5-year simulation illustrates the complex temporal relationships between the A/T/N components and CDR-SB, and demonstrates the disease-modifying potential of anti-amyloid therapy in early AD with an increasing clinical benefit over time.

## 2 | METHODS

The Q-ATN model is expressed in differential and algebraic equations that represent the four sequential linkages (L1–L4) between anti-amyloid treatment, A/T/N biomarkers, and CDR-SB. The rationale and mathematical expressions for each linkage, the data and sources used to calibrate and validate the model, and the methods used for parameter estimation and simulation are described in detail in the Supplementary Materials and Table S0, and summarized here. A graphical depiction of each linkage is given in Figure 1A–D respectively.

### 2.1 | L1 linkage: Anti-amyloid treatment reduces amyloid plaque

The L1 linkage (Figure 1A) combines the amyloid PET input function with the pharmacokinetics (PK) and pharmacodynamics (PD) of anti-amyloid therapy. In the untreated state, the rate of change (increase) of amyloid PET is represented by a parabolic input function that varies with the baseline amyloid PET level (left-upper graph of Figure 1A). The mean parameters of the parabola were estimated from published amyloid PET data<sup>17,18</sup> and an analysis of Alzheimer's Disease Neuroimaging Initiative (ADNI) data (Supplementary Material section S1.1 and references therein). The simulated increase of amyloid plaque during the untreated state, that is, natural history or placebo, is indicated by the green curve in the right graph of Figure 1A. During antibody treatment, the rate of change of amyloid PET corresponds to the difference between the input function and the rate of drug-induced amyloid removal, which depends on the PK and PD parameters and the dosing regimens for each antibody. Mean PK data for each of the anti-amyloid antibodies analyzed, that is, aducanumab, gantenerumab, lecanemab, bapineuzumab, and donanemab, were obtained from literature or unpublished Roche data and were modeled with two-compartment models representing intravenous or subcutaneous administration (details and references in Supplementary Material section S1.2). As an example, the simulated PK profile of a 10 mg/kg intravenous administration of aducanumab, given every 4 weeks, is illustrated in the left-middle graph of Figure 1A. The PD model for each antibody assumes a pseudo-first-order rate constant

for plaque removal ( $k_{DE}$ ) that is proportional to the plasma concentration, with an antibody-specific proportionality factor ( $\alpha_{rem}$ ) shown as the slope in the left-lower graph in Figure 1A. The  $\alpha_{rem}$  values were estimated for each antibody by fitting the time-course of mean amyloid PET data during treatment (Supplementary Materials section S1.3). The simulated 2-year time-course of amyloid PET for the 10 mg/kg aducanumab treatment is illustrated by the magenta curve in the right graph of Figure 1A.

## 2.2 | L2 linkage: Amyloid plaque modulates the production of excess (aggregated) tau

The L2 linkage (Figure 1B) connects amyloid PET levels to the time-course of tau PET standardized uptake value ratio (SUVR) levels, based on the longitudinal tau PET (floratacipir) versus amyloid PET data set from the Harvard Aging Brain Study (HABS) reported by Johnson et al.<sup>19</sup> and Sperling.<sup>20</sup> We assume that the elevated tau SUVR levels observed in the entorhinal cortex and inferior temporal cortex are the sum of a basal level ( $\approx 1.15$  SUVR) plus an excess level, resulting in a total maximum of  $\approx 2.8$  SUVR (Supplementary Materials section S2). Excess tau SUVR is assumed to represent aggregated tau, that is, intra- or extracellular filaments and neurofibrillary tangles.<sup>21</sup> A simulation of the HABS data set is illustrated by the family of sigmoidal curves shown in the lower graph of Figure 1B. These curves reflect the inter-subject variability seen in the HABS study (Supplementary Materials section S2)<sup>19,20</sup> and depend on a model parameter ( $Abeta_{50}$ ), which corresponds to the amyloid PET level at which an individual's tau SUVR curve crosses the midpoint between the basal and maximal levels (i.e., 50% of the difference). To generate these curves, the L2 linkage assumes that the production rate of excess tau SUVR ( $PR_{\tau}$ ) varies with the amyloid PET levels according to the family of dashed curves shown in the upper graph of Figure 1B. The  $PR_{\tau}$  curves also depend on  $Abeta_{50}$ , shifting to the right as  $Abeta_{50}$  increases.

The L2 linkage further assumes that aggregated tau is slowly eliminated by a first-order process with rate constant  $k_{\tau}$  (Supplementary Material section S2.1). Although the value of  $k_{\tau}$  cannot be inferred from the HABS data set or from other natural history studies, limited evidence from a transgenic mouse model of tauopathy<sup>22</sup> and cell culture studies<sup>23</sup> suggest that aggregated tau can be slowly degraded and eliminated from the brain, presumably via a microglial mechanism.<sup>24</sup> A nominal value of  $k_{\tau}$  ( $0.5 \text{ Yr}^{-1}$ ) was used in the present work and shown to be consistent with the half-life of aggregated tau in the transgenic mouse model using allometric scaling concepts (Supplementary Material section S2.2). A sensitivity analysis shows that  $k_{\tau}$  can influence the time-course of tau SUVR during anti-amyloid treatment as well as the downstream effects on CT and CDR-SB (Supplementary Material section S6). A longitudinal tau PET (floratacipir) study by Jack et al.<sup>25</sup> provides independent validation of the L2 linkage (Supplementary Material section S2.4).

## RESEARCH IN CONTEXT

- 1. Systematic review:** Published data and biologically plausible mechanisms were used to construct, calibrate, and validate a quantitative, semi-mechanistic model of Alzheimer's disease (AD) based on the amyloid/tau/neurodegeneration biomarker framework (the Q-ATN model) for simulating natural history and anti-amyloid treatment studies.
- 2. Interpretation:** Q-ATN model simulations were consistent with the time-course of clinical outcomes in natural history studies and also described the effects of several anti-amyloid antibodies observed in trials with positive and negative (or non-significant) clinical outcomes. A 5-year simulation of subcutaneous gantenerumab treatment illustrates the complex temporal relationships between the A/T/N biomarkers and predicts that the beneficial effects of continuous anti-amyloid treatment should increase markedly over time.
- 3. Future directions:** The current model prediction of the 27-month outcome of the gantenerumab Phase III GRADUATE studies will be assessed in late 2022. A population-based version of the Q-ATN model, informed by individual patient data, is currently in development.

## 2.3 | L3 linkage: Excess (aggregated) tau modulates cortical thinning

The L3 linkage (Figure 1C) relates the tau SUVR levels in the temporal cortex to the rate of cortical thinning ( $dCT/dt$ ) in the medial temporal cortex, a region that shows the greatest atrophy during early AD.<sup>6</sup> Based on La Joie et al.,<sup>26</sup> it is assumed that  $dCT/dt$  (expressed in mm/Yr) is proportional to the amount of excess tau, that is, tau SUVR  $- 1.15$ . A mean value for the proportionality factor  $S_{CT}$  ( $\approx 0.133 \text{ mm/Yr/SUVR}$ ) was estimated from Scott et al.,<sup>27</sup> Xie et al.,<sup>28</sup> and others (details and references in Supplementary Material section S3.1).

## 2.4 | L4 linkage: Cortical thickness determines CDR-SB

The L4 linkage (Figure 1D) relates the thickness of the medial temporal cortex (CT) to the clinical state (CDR-SB). Based on the magnetic resonance imaging (MRI) data of Dickerson et al.,<sup>29</sup> the empirical relationship between CT and CDR-SB is represented mathematically by a reverse sigmoidal function, truncated at the maximum possible value of 18. We assume that this relationship describes the longitudinal change of a population progressing from cognitively normal (CDR-SB = 0)

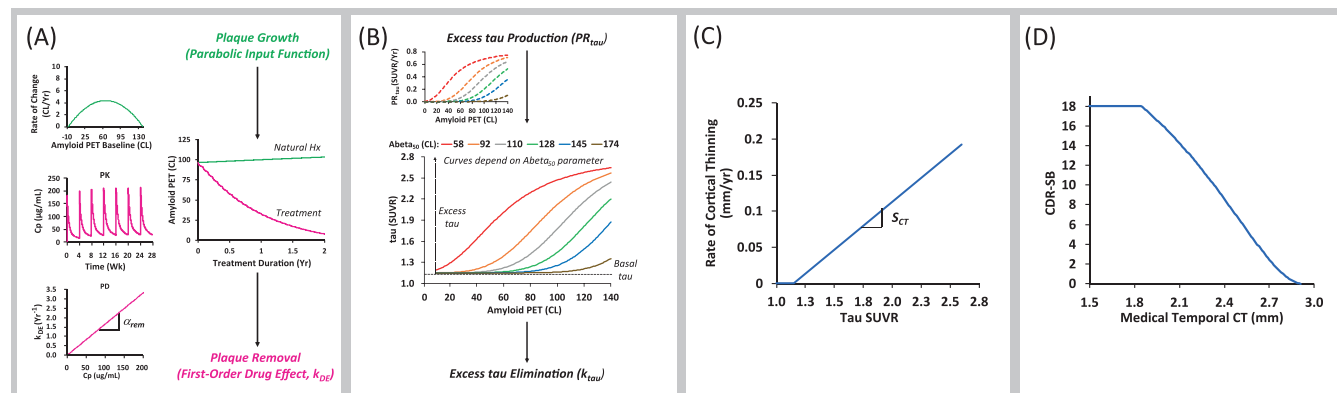


**FIGURE 1** Schematic representation of the four linkages (L1–L4) in the Q-ATN model. (A) L1 linkage connects anti-amyloid therapy to the dynamics of amyloid PET levels. (B) L2 linkage connects amyloid PET levels to the dynamics of tau PET SUVR. (C) L3 linkage connects tau PET SUVR to the rate of cortical thinning in the medial temporal cortex. (D) L4 linkage connects medial temporal cortical thickness to the CDR-SB. Tau SUVR data were calibrated to HABS data (entorhinal cortex and inferior temporal cortex ROIs; white matter reference).<sup>19,20</sup> See Methods for further explanations of the hypothesized mechanisms, experimental details, and the inserted graphs in each panel. CDR-SB, Clinical Dementia Rating – Sum of Boxes; CL, centiloid; Cp, plasma concentration; CT, cortical thickness; HABS, Harvard Aging Brain Study; Hx, history; PET, positron emission tomography; PK, pharmacokinetics; Q-ATN, quantitative amyloid/tau/neurodegeneration model; ROI, region of interest; SUVR, standardized uptake value ratio; Yr, year.

to AD, as the CT decreases from Dickerson's "older control" value of 2.91 mm to smaller values. The loss of neurons and their synaptic linkages in the medial temporal cortex (and other brain regions) is presumably responsible for the cognitive and functional impairments that are quantified by the CDR-SB.<sup>30</sup> The modeled curve is in good agreement with Dickerson's data in four patient groups (Supplementary Material section S4.1). Additional CDR-SB data from the 5-year longitudinal study of Williams et al.<sup>8</sup> were also used to calibrate the L4 linkage (see Results). Although Williams et al. did not measure CT, the time-course of mean CDR-SB, which reaches values of  $\approx 15$  in their mild AD group, helps to constrain the relationship between CT and CDR-SB at the higher CDR-SB values.

## 2.5 | Validation of the model

The first validation step compared Q-ATN simulations of CDR-SB with data from natural history studies, that is, analysis of ADNI data (Delor et al.)<sup>9</sup> and a combined data set of patients across the AD spectrum (Kim et al.)<sup>10</sup> (Supplementary Material section S5.1).

The second validation step compared Q-ATN simulations of amyloid PET and CDR-SB with reported data from the aducanumab EMERGE trial, and simulations of tau PET to data from the Phase III tau PET sub-study (Supplementary Material section S5.2).<sup>11,31</sup>

The third validation step compared Q-ATN simulations of amyloid PET and CDR-SB for other anti-amyloid antibodies based on reported clinical trial data from 13 active treatment arms.<sup>12–15,32</sup> Validation of the model was assessed by the concordance of these simulations and the observed placebo-corrected differences of amyloid PET and CDR-SB (Supplementary Material section S5.3).

## 2.6 | Five-year simulation of gantenerumab treatment

Simulated 5-year trajectories of amyloid PET, tau PET, CT, and CDR-SB were based on the gantenerumab dosing regimen applied in the 27-month (116-week) Phase III GRADUATE studies,<sup>16</sup> with continuation of the target dose regimen to Year 5 (Supplementary Material section S6). Model parameters were adjusted so that the simulation matched the mean baseline values of amyloid PET and CDR-SB reported for the GRADUATE studies.<sup>16,33</sup> An approximate estimate of the uncertainty in the trajectories of amyloid PET and CDR-SB is provided (Supplementary Material section S6).

## 2.7 | Model parameter estimates

A complete listing of the model parameter estimates and the methods used to derive them is given in Supplementary Material section S7.

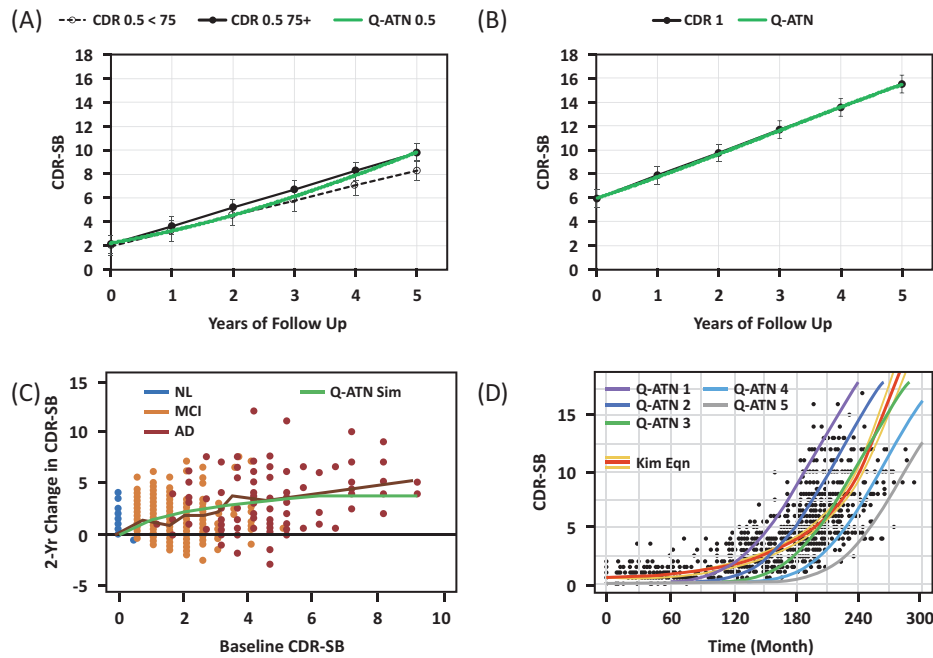


**FIGURE 2** Comparison of Q-ATN model simulations to data from natural history studies. (A) Data points correspond to the mean CDR-SB values in patients with baseline global CDR of 0.5 from the 5-year study by Williams et al.<sup>8</sup> stratified by age (solid line and filled circles: age <75 years; dashed line and open circles: age ≥75 years). Green curve corresponds to Q-ATN simulation for entire population. (B) Data points correspond to the mean CDR-SB values in patients with baseline global CDR of 1 from the 5-year study by Williams et al.<sup>8</sup> Green curve corresponds to Q-ATN simulation. (C) Data points correspond to the 2-year change in CDR-SB versus the baseline CDR-SB; figure adapted (with permission) from Delor's analysis of ADNI data.<sup>9</sup> Brown curve is Loess function describing trend of all data. Green curve corresponds to Q-ATN simulation. (D) Data points correspond to CDR-SB versus time (months) from the combined data set compiled by Kim et al.<sup>10</sup> Brown curve is the predictive equation of Kim et al. describing the entire data set. Q-ATN simulations are denoted Q-ATN 1 to Q-ATN 5. The five simulations correspond to different initial values of amyloid PET: Q-ATN 1 (42.4 CL), Q-ATN 2 (34.8 CL), Q-ATN 3 (27.9 CL), Q-ATN 4 (21.8 CL), and Q-ATN 5 (16.5 CL). See Supplementary Material section S5.1 for details. AD, Alzheimer's disease; ADNI, Alzheimer's Disease Neuroimaging Initiative; CDR, Clinical Dementia Rating; CDR-SB, Clinical Dementia Rating – Sum of Boxes; CL, centiloid; MCI, mild cognitive impairment; NL, normal; Q-ATN, quantitative amyloid/tau/neurodegeneration model.

### 3 | RESULTS

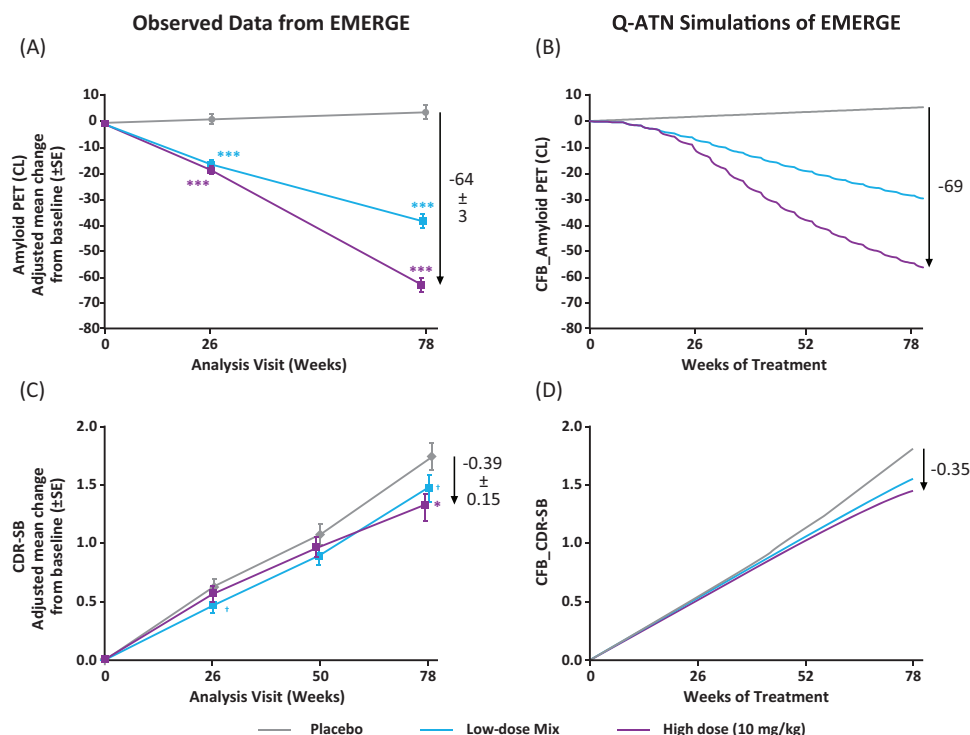
#### 3.1 | Natural history studies: Calibration and first validation step

Figure 2 compares Q-ATN simulations with data from three natural history studies. The Q-ATN simulations (green curves) agree well with the 5-year CDR-SB data from Williams et al. in patients with global CDR scores of 0.5 (Figure 2A) and 1 (Figure 2B),<sup>8</sup> which were used to calibrate the L4 linkage. A greater rate of increase in CDR-SB is seen in the latter population (Figure 2B). In Figure 2C, validation data from three subpopulations (normal, MCI, and AD) in the ADNI study<sup>9</sup> show the dependence of the 2-year change in CDR-SB versus the baseline value. The Loess function describing these data (brown curve) increases with baseline CDR-SB and is in very good agreement with the Q-ATN simulation (green curve). Finally, Figure 2D shows the combined CDR-SB data set from Kim et al. spanning 300 months of disease progression.<sup>10</sup> Superimposed on these data are five simulated curves that shift from left to right as the amyloid PET level at time 0 decreases from 42.4 CL to 16.5 CL (see legend of Figure 2);  $A\beta_{50}$  was the same (110 CL) for all curves. Except for the early months, the Q-ATN simulations appear

to capture the characteristic time-course of the data set and account for much of the variation by the different initial amyloid PET levels.

#### 3.2 | Comparison of simulated and observed clinical data from the EMERGE trial and tau PET sub-study: Second validation step

Figure 3 provides side-by-side comparisons of the Q-ATN simulations with observed data on amyloid PET and CDR-SB from the 78-week Phase III EMERGE trial of aducanumab.<sup>11,31</sup> The observed baseline-subtracted time-course of the amyloid PET data (mean ± standard error of the mean [SEM]) (Figure 3A) is described well by the Q-ATN simulations (Figure 3B), with a small increase in the placebo group and marked decreases for the low-dose mixture and high-dose groups, respectively. At Week 78, the Q-ATN value of the placebo-corrected difference in the high-dose group (−69 CL) is comparable to the observed value (−64 ± 3 CL). More importantly, the observed baseline-subtracted CDR-SB trajectories (Figure 3C) are also well described by the Q-ATN simulations (Figure 3D). At Week 78, the Q-ATN value of the placebo-corrected difference in the high-dose group (−0.35 units)



**FIGURE 3** Side-by-side comparison of observed time-course of amyloid PET and CDR-SB and the respective Q-ATN simulations from the EMERGE trial of aducanumab. (A) Observed mean  $\pm$  SEM data of baseline-subtracted amyloid PET levels (converted from SUVR to CL) for the placebo, low-dose mixture, and high-dose groups.<sup>11,31</sup> \*\*\*  $p < 0.001$ . (B) Q-ATN simulation of the amyloid PET data. (C) Observed mean  $\pm$  SEM data of baseline-subtracted CDR-SB values for the placebo, low-dose mixture, and high-dose groups.<sup>11,31</sup>  $\dagger 0.05 < p < 0.1$ ; \*  $p < 0.05$ . (D) Q-ATN simulation of the CDR-SB data. Downward arrows and values ( $\pm$  SEM) correspond to the end of study placebo-corrected difference of the high-dose group in the observed and simulated data. See Supplementary Material section S5.2.1 for details. CDR-SB, Clinical Dementia Rating – Sum of Boxes; CFB, change from baseline; CL, centiloid; PET, positron emission tomography; Q-ATN, quantitative amyloid/tau/neurodegeneration model; SEM, standard error of mean.

is close to the observed value ( $-0.39 \pm 0.16$  units). Figure 4 compares Q-ATN simulations with observed data from the small tau PET sub-study in 36 subjects from the Phase III ENGAGE and EMERGE trials.<sup>31</sup> The mean baseline-subtracted changes of tau PET from the medial temporal composite (Figure 4A) are directionally the same as the Q-ATN simulations (Figure 4B) for the placebo, the low-dose, and the two high-dose regimens (6 mg/kg and 10 mg/kg). The linear correlation of the change in tau PET versus cumulative dose shown for individual subjects (Figure 4C) is very similar to the linear correlation derived from the Q-ATN simulation of the four dose groups (Figure 4D).

### 3.3 | Comparison of simulated and observed data from five anti-amyloid antibodies: Third validation step

Figures 5A and 5B compare Q-ATN simulations of amyloid PET and CDR-SB, respectively, with observed data from five anti-amyloid antibodies studied in double-blind Phase II or III trials (13 active treatment arms). For amyloid PET (Figure 5A), the simulated placebo-corrected change from baseline levels at the end of the study is in excellent agreement with the observed data for all treatment arms ( $R^2 = 0.972$ ;

$p < 0.0001$ ). This is as expected given that the drug-specific  $\alpha_{rem}$  parameters of the L1 linkage were calibrated with amyloid PET data from the same clinical trials (other than aducanumab). Of greater significance, the corresponding simulated placebo-corrected changes of CDR-SB (Figure 5B) are in generally good agreement with the observed data ( $R^2 = 0.606$ ;  $p < 0.01$ ), falling within 1 SEM of the observed means for most of the 13 treatment arms. Notable exceptions were the 225 mg dose group of the SCarlet RoAD study and the high-dose treatment group of the ENGAGE study, both of which exhibited smaller observed treatment effects than predicted. Finally, Figure 5C plots the simulated data of Figure 5B versus the simulated data of Figure 5A to emulate the FDA's graph of clinical effect versus amyloid plaque removal.<sup>1</sup> The resulting plot shows a highly significant correlation ( $R^2 = 0.880$ ;  $p < 0.0001$ ).

### 3.4 | Five-year simulation of gantenerumab treatment

Figure 6 shows Q-ATN simulations of amyloid PET, tau PET, CT, and CDR-SB for a hypothetical 5-year, placebo-controlled study of subcutaneous gantenerumab. The simulation uses the same titration regimen

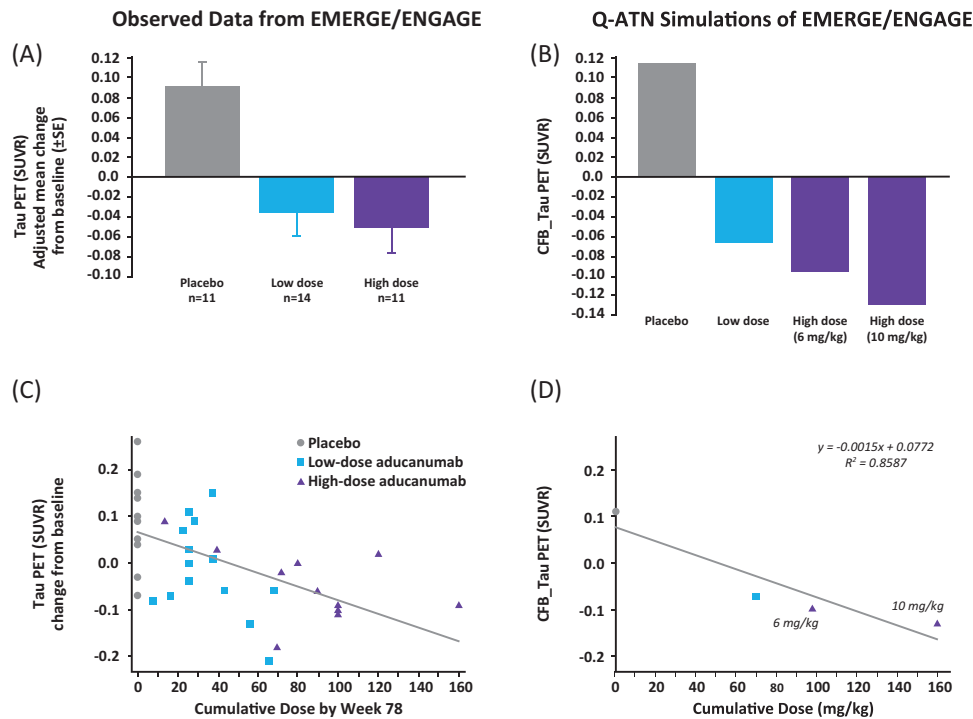


**FIGURE 4** Side-by-side comparison of observed tau PET data in the medial temporal region of interest and the respective Q-ATN simulations from the combined tau PET sub-study of the EMERGE and ENGAGE trials of aducanumab. (A) Observed mean  $\pm$  SEM change from baseline in tau PET SUVR for the placebo, low-dose, and high-dose groups.<sup>31</sup> \*\*\*  $p < 0.001$ . (B) Q-ATN simulations of change from baseline in tau PET SUVR for placebo (gray bar), low dose-mixture (blue bar), and two high-dose regimens corresponding to 6 mg/kg (left magenta bar) and 10 mg/kg (right magenta bar) target doses. (C) Observed scatter plot of individual subjects' change from baseline in tau PET SUVR versus the cumulative dose received by Week 78.<sup>31</sup> Data points are identified by treatment groups: placebo (gray filled circles); low-dose (blue filled squares); and high-dose (magenta filled triangles). Correlation line is shown in gray. (D) Q-ATN simulations of change from baseline in tau PET SUVR for placebo, low dose-mixture, and two high-dose regimens corresponding to 6 mg/kg and 10 mg/kg target doses plotted versus the cumulative dose received by Week 78 per protocol. Regression line is shown in gray with equation and  $R^2$  in upper right. Observed tau SUVR data were obtained with tau tracer MK-6240 (medial temporal composite; cerebellar gray reference). Simulated tau SUVR data were calibrated to HABS data (entorhinal cortex and inferior temporal cortex ROIs; white matter reference).<sup>19,20</sup> See Supplementary Material section S5.2.1 for details. CFB, change from baseline; HABS, Harvard Aging Brain Study; PET, positron emission tomography; Q-ATN, quantitative amyloid/tau/neurodegeneration model; ROI, region of interest; SEM, standard error of mean; SUVR, standardized uptake value ratio.

currently applied in the 27-month GRADUATE Phase III trials,<sup>16</sup> and continues the target dose (510 mg every 2 weeks) until Year 5. On a monthly basis, the target dose is more than 5-fold higher than that used in the Phase III SCarlet RoAD and Marguerite RoAD studies (Figure 5). The simulated amyloid PET levels increase from  $\approx 89$  to  $\approx 116$  CL in the placebo group and decrease to very low levels with treatment, a placebo-corrected change of  $-111$  CL (Figure 6A). After a slight time lag, the tau PET levels show a similar pattern in the treated group (Figure 6B). The placebo group shows a steady decrease in the thickness of the medial temporal cortex, whereas the treatment group shows an upward bending of the curve, starting at about 1.5 years (Figure 6C). Conversely, the CDR-SB shows a steady increase in the placebo group, whereas the treatment shows a downward bending of the curve after 1.5 years (Figure 6D). At 5 years, the placebo-corrected change in CDR-SB is predicted to be  $-5.2$  points; while at 27 months, the simulated treatment effect is predicted to be  $-0.87$  points. Based on a sensitivity analysis of the parameter  $k_{\text{tau}}$ , the uncertainties in these predictions are estimated to be  $\approx 15\%$  and  $\approx 25\%$ , respectively (Supplementary Material section S6).

## 4 | DISCUSSION

Based on experimental data and plausible biological concepts, the Q-ATN model quantifies four hypothesized linkages between anti-amyloid treatment and clinical outcome. Although other mathematical models of AD have been proposed,<sup>34-43</sup> the Q-ATN model is the first to link antibody-induced amyloid plaque removal, A/T/N biomarkers, and CDR-SB. The key assumptions, overall behavior of the model, and its limitations are discussed below.

Linkage 1 is based on the parabolic input function for amyloid plaque as well as the PKPD model of the drug effect on plaque removal. The former is well supported by human data and accounts for the sigmoidal increase in amyloid PET with time.<sup>17,18</sup> A mechanistic interpretation of the parabolic input function is offered in Supplementary Material section S1.1. The drug-specific proportionality factors ( $\alpha_{\text{rem}}$  values) relating plasma levels to the pseudo-first-order drug effect ( $k_{\text{DE}}$ ), provide a simple means for quantifying and comparing amyloid plaque removal between antibodies. From a mechanistic perspective,  $\alpha_{\text{rem}}$  is a hybrid parameter, incorporating the permeation of antibody across the

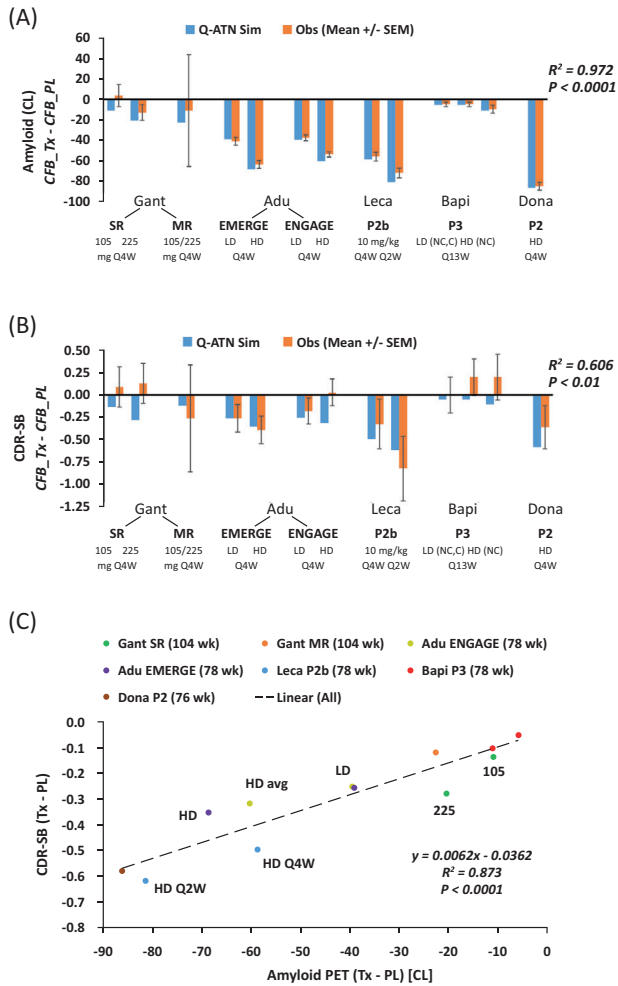


**FIGURE 5** Comparison of the observed placebo-corrected changes with Q-ATN simulations of amyloid PET and CDR-SB for five anti-amyloid antibodies (13 active treatment arms). Data correspond to gantenerumab SR and MR double-blind trials (subcutaneous Q4W doses in mg), aducanumab EMERGE and ENGAGE trials (low-dose [LD] and high-dose [HD] regimens), lecanemab (Leca) Phase II (10 mg/kg Q4W and Q2W regimens), bapineuzumab (Bapi) Phase III (LD for APOE  $\epsilon$ 4 non-carriers [NC] and carriers [C] and HD for NC), and donanemab Phase II (HD regimen). (A) Observed mean  $\pm$  SEM amyloid PET data (orange bars) and Q-ATN simulations (blue bars).  $R^2$  and  $p$ -value of the correlation are shown to the right. (B) Observed mean  $\pm$  SEM CDR-SB (orange bars) and Q-ATN simulations (blue bars).  $R^2$  and  $p$ -value of the correlation are shown to the right. (C) Correlation plot of simulated placebo-corrected changes in CDR-SB versus simulated placebo-corrected changes in amyloid PET for all 13 treatment arms shown in panels (A) and (B). Duration of each study given in legend. Dashed regression line is shown with equation,  $R^2$ , and  $p$ -value. See Supplementary Material section 55.3 for details and data references. Adu, aducanumab; APOE, apolipoprotein E; Bapi, bapineuzumab; C, carriers; CDR-SB, Clinical Dementia Rating – Sum of Boxes; CFB\_PL, change from baseline in the placebo arm; CFB\_Tx, change from baseline in the treatment arm; CL, centiloid; Dona, donanemab; Gant, gantenerumab; HD, high dose; Leca, lecanemab; LD, low dose; MR, Marguerite RoAD; NC, non-carriers; P2(b), Phase II(b); P3, Phase III; PET, positron emission tomography; Q2W, every two weeks; Q4W, every four weeks; Q13W, every 13 weeks; Q-ATN, quantitative amyloid/tau/neurodegeneration model; SEM, standard error of mean; SR, SCarlet RoAD; wk, week.

blood-brain barrier, its binding to amyloid plaque, and its activation of microglia, which are assumed to phagocytize and clear plaque.<sup>44</sup>

Linkage 2 is the most complex in the model. Based on data from the HABS study, it is hypothesized that amyloid plaque levels (expressed in CL) reversibly modulate the production rate of excess (aggregated) tau SUVR measured in the temporal lobe. Variability in this relationship is controlled by the model parameter  $Abeta_{50}$ . The influence of amyloid plaque on tau aggregation could result from the enhanced phosphorylation of tau species as well as other potential mechanisms.<sup>45,46</sup> The pathophysiological mechanisms that determine  $Abeta_{50}$  and its variability are presently unknown. It is also assumed that a first-order process (with rate constant  $k_{tau}$ ) slowly eliminates aggregated tau. Estimating the value of  $k_{tau}$  is difficult, as it cannot be inferred directly from natural history studies. The current  $k_{tau}$  value ( $0.5 \text{ Yr}^{-1}$ ) is consistent with prior estimates<sup>35</sup> and preclinical data.<sup>22</sup> It also accounts well for the observed tau PET data in the EMERGE and ENGAGE trials, and the trends in the medial temporal tau SUVR reported for donanemab.<sup>47</sup>

Linkage 3 is supported by natural history data showing a linear correlation between tau PET levels and the rate of thinning of the medial temporal cortex and other regions of interest. We assume this is a causal and reversible relationship, that is, that the rate of thinning will increase or decrease as the excess tau SUVR increases or decreases. In the 5-year Q-ATN simulation for subcutaneous gantenerumab treatment, the placebo-corrected difference in medial temporal CT at the 27-month endpoint of the GRADUATE studies is only 0.04 mm; too small to be detected with current MRI methods.<sup>48</sup> Although previous studies of anti-amyloid therapy by active immunization (AN1792), bapineuzumab, low-dose gantenerumab, donanemab, lecanemab, and aducanumab have reported small decreases in whole-brain volume that were (in some reports) larger than that seen in the placebo group,<sup>11,12,14,15,49,50</sup> no significant differences between active and placebo groups were reported for the hippocampal volume, except for bapineuzumab (which removed negligible amounts of plaque).<sup>50</sup> Because the hippocampus contributes to the medial temporal CT, the lack of adverse treatment effects suggests that the phenomenon of “pseudo-atrophy” attributed to the changes in whole-brain volume,<sup>49,51</sup> may not be relevant to our simulations.

Linkage 4 was calibrated by Dickerson's mean data on medial temporal thickness and CDR-SB in four patient subgroups,<sup>29</sup> and the natural history study of Williams et al. that extends to higher CDR-SB values.<sup>8</sup> Although the biological assumption appears sound, more longitudinal data would greatly strengthen this linkage.

Based on these four linkages, the current Q-ATN model is able to connect amyloid plaque increase or removal to the time-course of CDR-SB in natural history and anti-amyloid therapy studies, respectively. The similarity between the Q-ATN simulations of the EMERGE study and the observed data are particularly noteworthy, especially the close correspondence of the simulations to the CDR-SB and tau PET data. The model also accounts reasonably well for the observed treatment effects reported in Phase II and III studies conducted with other anti-amyloid antibodies targeting plaques and fibrillary forms of amyloid.

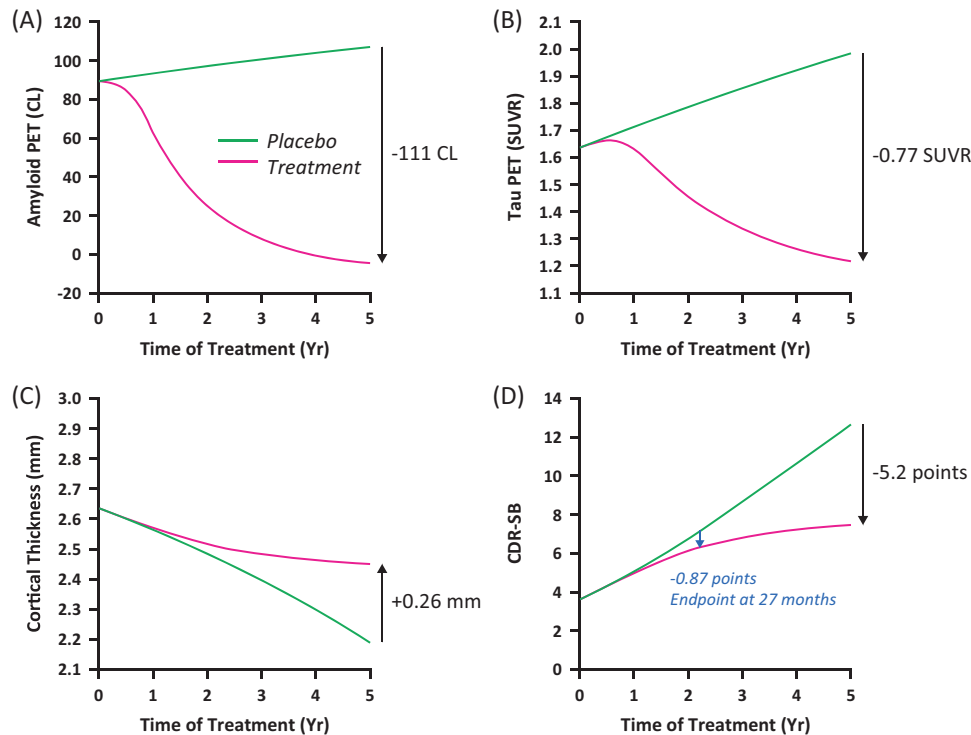


**FIGURE 6** Q-ATN simulations of (A) amyloid PET, (B) tau PET, (C) cortical thickness, and (D) CDR-SB, respectively, for a hypothetical 5-year, placebo-controlled study with subcutaneous gantenerumab treatment. Placebo (natural history) shown in green; treatment (based on the titration regimen<sup>16</sup> in GRADUATE studies) shown in magenta. Black arrows and numbers correspond to the placebo-corrected changes in each variable at the 5-year time point. Blue arrow and number (panel D) shows the placebo-corrected change in CDR-SB at the 27-month endpoint of the GRADUATE studies. Values of amyloid PET and CDR-SB at time = 0 derived from baseline data reported for the GRADUATE studies.<sup>16,33</sup> Tau SUVR data were calibrated to HABS data (entorhinal cortex and inferior temporal cortex ROIs; white matter reference).<sup>19,20</sup> See Supplementary Materials section S6 for details. CDR-SB, Clinical Dementia Rating – Sum of Boxes; CL, centiloid; HABS, Harvard Aging Brain Study; PET, positron emission tomography; ROI, region of interest; SUVR, standardized uptake value ratio; Yr, year.

Based on the dosing regimen used in the ongoing GRADUATE studies, the 5-year simulation of subcutaneous gantenerumab treatment illustrates the expected time-course of a disease-modifying treatment, with longer treatment duration leading to greater clinical benefit. The accuracy of the predicted treatment effects at the 27-month time point will be assessed at the conclusion of the GRADUATE studies, anticipated for late 2022.<sup>16</sup>

The major limitation of the present Q-ATN model is the sparsity of available data needed for rigorous parameter estimation, particularly in linkages L2–L4, and the necessity of combining information from diverse studies. Moreover, the current model only describes mean behavior without accounting for inter-subject variability and does not represent the mechanisms of the spatial spread of amyloid and tau.<sup>36,39,41</sup> Real-world factors, such as missed dosing, unequal distributions of fast and slow progressors, and the potential effects of the COVID pandemic are also not accounted for in the present model.<sup>52</sup> To this end, a population-based version of the Q-ATN model incorporating actual dosing regimens, PK and PD modeling of gantenerumab, and inter-subject variability in model parameters is currently in development.

## ACKNOWLEDGMENTS

Norman A. Mazer thanks Roche colleagues Roxana Aldea, Marzia Scelsi, Kaycee Sink, and Matteo Tonietto; and modelers Clement Abi Nader of Université Côte d'Azur and Matthias Machacek of LYO-X GmbH for helpful discussions on the Q-ATN model. Data collection and sharing for this project was funded by the Alzheimer's Disease Neuroimaging Initiative (ADNI; National Institutes of Health Grant U01 AG024904) and Department of Defense ADNI (DOD ADNI; Department of Defense award number W81XWH-12-2-0012). ADNI is funded by the National Institute on Aging, the National Institute of Biomedical Imaging and Bioengineering, and through generous contributions from the following: AbbVie; Alzheimer's Association; Alzheimer's Drug Discovery Foundation; Araclon Biotech; BioClinica, Inc.; Biogen; Bristol Myers Squibb; CereSpir, Inc.; Cogstate; Eisai, Inc.; Elan Pharmaceuticals, Inc.; Eli Lilly and Company; EuroImmun; F. Hoffmann-La Roche Ltd and its affiliated company Genentech, Inc.; Fujirebio; GE Healthcare; IXICO Ltd; Janssen Alzheimer Immunotherapy Research & Development, LLC; Johnson & Johnson Pharmaceutical Research & Development LLC; Lumosity; Lundbeck; Merck & Co., Inc.; Meso Scale Diagnostics, LLC; NeuroRx Research; Neurotrack

Technologies; Novartis Pharmaceuticals Corporation; Pfizer, Inc.; Piramal Imaging; Servier; Takeda Pharmaceutical Company; and Transition Therapeutics. The Canadian Institutes of Health Research is providing funds to support ADNI clinical sites in Canada. Private sector contributions are facilitated by the Foundation for the National Institutes of Health ([www.fnih.org](http://www.fnih.org)). The grantee organization is the Northern California Institute for Research and Education, and the study is coordinated by the Alzheimer's Therapeutic Research Institute at the University of Southern California. ADNI data are disseminated by the Laboratory for Neuro Imaging (LONI) at the University of Southern California. This study was funded by F. Hoffmann-La Roche Ltd, Basel, Switzerland. Beyond employment of the authors, F. Hoffmann-La Roche Ltd had no role in the study design, collection, analysis and interpretation of data, and the writing of the report. The corresponding author had full access to all the data needed for the conduct of the work and had final responsibility for the decision to submit for publication. Editorial support was provided by Rachel Johnson, PhD, of Nucleus Global, funded by F. Hoffmann-La Roche Ltd.

### CONFLICTS OF INTEREST

N.A.M., C.H., D.L., G.K., F.B., H.P.G., G.A.K., and M.B.K. are full-time employees of F. Hoffmann-La Roche Ltd. R.G. was a full-time employee of F. Hoffmann-La Roche Ltd at the time of this work and is currently acting as a consultant for F. Hoffmann-La Roche Ltd. R.S.D. is an employee of F. Hoffman-La Roche Ltd and Genentech Inc. J.S. is an employee of Roche Products Ltd. N.A.M., G.K., F.B., and M.B.K. have received support for attending meetings and/or travel from F. Hoffmann-La Roche Ltd. N.A.M., C.H., G.K., F.B., and M.B.K. disclose involvement in patents related to their employment. G.A.K. discloses participation in data safety monitoring board/advisory board for University of California, San Francisco, CA, US. N.A.M., C.H., D.L., R.G., G.K., F.B., H.P.G., G.A.K., M.B.K., J.S., and R.S.D. own stock or have stock options in F. Hoffmann-La Roche Ltd. Author disclosures are available in the [supporting information](#).

### ORCID

Norman A. Mazer  <https://orcid.org/0000-0003-3759-0115>

### REFERENCES

- Center for Drug Evaluation and Research (CDER). Application Number: 761178Orig1s000 (Aduhelm). Clinical Pharmacology and Biopharmaceutics Review(s). Accessed July 14, 2022. [https://www.accessdata.fda.gov/drugsatfda\\_docs/nda/2021/761178Orig1s000ClinPharm\\_Redacted.pdf](https://www.accessdata.fda.gov/drugsatfda_docs/nda/2021/761178Orig1s000ClinPharm_Redacted.pdf)
- Alzheimer's Drug Discovery Foundation. FDA breakthrough therapy designation for two more Alzheimer's drugs demonstrates promise of pipeline. Accessed July 14, 2022. <https://www.alzdiscovery.org/newsroom/announcements/fda-breakthrough-therapy-designation-for-two-more-alzheimers-drugs-demonstrates-promise-of-pipeline>
- Inacio P. Today Alzheimer's News, FDA Grants Breakthrough Therapy Designation to Gantenerumab. Accessed July 14, 2022. <https://alzheimersnewstoday.com/news/gantenerumab-alzheimers-named-fda-breakthrough-therapy/>
- Steinbrook R. The accelerated approval of aducanumab for treatment of patients with Alzheimer disease. *JAMA Int Med.* 2021;181:1281.
- Selkoe DJ, Hardy J. The amyloid hypothesis of Alzheimer's disease at 25 years. *EMBO Mol Med.* 2016;8:595-608.
- Jack CR Jr, Bennett DA, Blennow K, et al. A/T/N: an unbiased descriptive classification scheme for Alzheimer disease biomarkers. *Neurology.* 2016;87:539-547.
- Jack CR Jr, Bennett DA, Blennow K, et al. NIA-AA Research Framework: toward a biological definition of Alzheimer's disease. *Alzheimers Dement.* 2018;14:535-562.
- Williams MM, Storandt M, Roe CM, Morris JC. Progression of Alzheimer's disease as measured by Clinical Dementia Rating Sum of Boxes scores. *Alzheimers Dement.* 2013;9:S39-44.
- Delor I, Charoin JE, Gieschke R, Retout S, Jacqmin P. Modeling Alzheimer's disease progression using disease onset time and disease trajectory concepts applied to CDR-SOB scores from ADNI. *CPT Pharmacometrics Syst Pharmacol.* 2013;2:e78.
- Kim KW, Woo SY, Kim S, et al. Disease progression modeling of Alzheimer's disease according to education level. *Sci Rep.* 2020;10:16808.
- Budd Haeberlein S, Aisen PS, Barkhof F, et al. Two randomized phase 3 studies of aducanumab in early Alzheimer's disease. *J Prev Alzheimers Dis.* 2022;9:197-210.
- Ostrowitzki S, Lasser RA, Dorflinger E, et al. A phase III randomized trial of gantenerumab in prodromal Alzheimer's disease. *Alzheimers Res Ther.* 2017;9:95.
- Swanson CJ, Zhang Y, Dhadda S, et al. A randomized, double-blind, phase 2b proof-of-concept clinical trial in early Alzheimer's disease with lecanemab, an anti-A $\beta$  protofibril antibody. *Alzheimers Res Ther.* 2021;13:80.
- Salloway S, Sperling R, Fox NC, et al. Two phase 3 trials of bapineuzumab in mild-to-moderate Alzheimer's disease. *N Engl J Med.* 2014;370:322-333.
- Mintun MA, Lo AC, Duggan Evans C, et al. Donanemab in early Alzheimer's disease. *N Engl J Med.* 2021;384:1691-1704.
- Lane C, Bullain S, Thanasopoulou A, et al. ROC12: baseline characteristics of the GRADUATE studies: phase III randomized, placebo-controlled studies investigating subcutaneous gantenerumab in participants with early Alzheimer's disease. *J Prev Alzheimers Dis.* 2021;8:S45-6.
- Jack CR Jr, Wiste HJ, Lesnick TG, et al. Brain  $\beta$ -amyloid load approaches a plateau. *Neurology.* 2013;80:890-896.
- Villemagne VL, Burnham S, Bourgeat P, et al. Amyloid  $\beta$  deposition, neurodegeneration, and cognitive decline in sporadic Alzheimer's disease: a prospective cohort study. *Lancet Neurol.* 2013;12:357-367.
- Johnson K, Jacobs H, Hansseuw B, et al. Critical threshold of elevated amyloid associated with rapid tau accumulation: a ca-tau-strophe in the making. Presentation at the Human Amyloid Imaging (HAI) Conference; Miami, FL, USA; January 15-17, 2020.
- Sperling R. The AT(N) Framework: progression from cognitively unimpaired to mild cognitive impairment. Presentation at the Mild Cognitive Impairment (MCI) Symposium; Miami, FL, USA; January 18-19, 2020.
- Leuzy A, Chiotis K, Lemoine L, et al. Tau PET imaging in neurodegenerative tauopathies – still a challenge. *Mol Psychiatry.* 2019;24:1112-1134.
- Yamada K, Patel TK, Hochgräfe K, et al. Analysis of in vivo turnover of tau in a mouse model of tauopathy. *Mol Neurodegener.* 2015;10:55.
- Croft CL, Goodwin MS, Ryu DH, et al. Photodynamic studies reveal rapid formation and appreciable turnover of tau inclusions. *Acta Neuropathol.* 2021;141:359-381.
- Das R, Balmik AA, Chinnathambi S. Phagocytosis of full-length Tau oligomers by Actin-remodeling of activated microglia. *J Neuroinflammation.* 2020;17:10.
- Jack CR Jr, Wiste HJ, Schwarz CG, et al. Longitudinal tau PET in ageing and Alzheimer's disease. *Brain.* 2018;141:1517-1528.

26. La Joie R, Visani AV, Baker SL, et al. Prospective longitudinal atrophy in Alzheimer's disease correlates with the intensity and topography of baseline tau-PET. *Sci Transl Med*. 2020;12:eau5732.
27. Scott MR, Hampton OL, Buckley RF, et al. Inferior temporal tau is associated with accelerated prospective cortical thinning in clinically normal older adults. *Neuro Image*. 2020;220:116991.
28. Xie L, Das SR, Wisse LEM, Ittyerah R, Yushkevich PA, Wolk DA. Early tau burden correlates with higher rate of atrophy in transentorhinal cortex. *J Alzheimers Dis*. 2018;62:85-92.
29. Dickerson BC, Bakkour A, Salat DH, et al. The cortical signature of Alzheimer's disease: regionally specific cortical thinning relates to symptom severity in very mild to mild AD dementia and is detectable in asymptomatic amyloid-positive individuals. *Cereb Cortex*. 2009;19:497-510.
30. Morris JC. The Clinical Dementia Rating (CDR): current version and scoring rules. *Neurology*. 1993;43:2412-2414.
31. Budd Haerberlein S, von Hehn C, Tian Y, et al. EMERGE and ENGAGE topline results: two phase 3 studies to evaluate aducanumab in patients with early Alzheimer's disease. Presentation at the Clinical Trials on Alzheimer's Disease (CTAD) Annual Conference; San Diego, CA, USA; December 4-7, 2019.
32. Swanson CJ, Zhang Y, Dhadda S, et al. Clinical and biomarker updates from BAN2401 study 201 in early AD. Presentation at the Clinical Trials on Alzheimer's Disease (CTAD) Annual Conference; Barcelona, Spain; October 24-27, 2018.
33. Klein G, Delmar P, Voyle N, et al. Concordance of visual and quantitative assessments of baseline amyloid scans in the GRADUATE gantenerumab studies. Presentation at the Human Amyloid Imaging (HAI) Conference; Miami, FL, USA; January 15-17, 2020.
34. Edelstein-Keshet L, Spiros A. Exploring the formation of Alzheimer's disease senile plaques in silico. *J Theor Biol*. 2002;216:301-326.
35. Hao W, Friedman A. Mathematical model on Alzheimer's disease. *BMC Syst Biol*. 2016;10:108.
36. Kuznetsov IA, Kuznetsov AV. Simulating the effect of formation of amyloid plaques on aggregation of tau protein. *Proc Math Phys Eng Sci*. 2018;474:20180511.
37. Geerts H, Spiros A. Learning from amyloid trials in Alzheimer's disease. A virtual patient analysis using a quantitative systems pharmacology approach. *Alzheimers Dement*. 2020;16:862-872.
38. Raket LL. Statistical disease progression modeling in Alzheimer disease. *Front Big Data*. 2020;3:24.
39. Bertsch M, Franchi B, Meschini V, Tesi MC, Tosin A. A sensitivity analysis of a mathematical model for the synergistic interplay of amyloid beta and tau on the dynamics of Alzheimer's disease. *Brain Multiphys*. 2021;2:100020.
40. Abi Nader C, Ayache N, Frisoni GB, Robert P, Lorenzi M, Alzheimer's Disease Neuroimaging Initiative. Simulating the outcome of amyloid treatments in Alzheimer's disease from imaging and clinical data. *Brain Commun*. 2021;3:fcab091.
41. Schäfer A, Peirlinck M, Linka K, Kuhl E, Alzheimer's Disease Neuroimaging Initiative (ADNI). Bayesian physics-based modeling of tau propagation in Alzheimer's disease. *Front Physiol*. 2021;12:702975.
42. Tahami Monfared AA, Byrnes MJ, White LA, Zhang Q. Alzheimer's disease: epidemiology and clinical progression. *Neurol Ther*. 2022;11:553-569.
43. Karelina T, Lerner S, Stepanov A, Meerson M, Demin O. Monoclonal antibody therapy efficacy can be boosted by combinations with other treatments: predictions using an integrated Alzheimer's disease platform. *CPT Pharmacometrics Syst Pharmacol*. 2021;10:543-550.
44. Bohrmann B, Baumann K, Benz J, et al. Gantenerumab: a novel human anti-A $\beta$  antibody demonstrates sustained cerebral amyloid- $\beta$  binding and elicits cell-mediated removal of human amyloid- $\beta$ . *J Alzheimers Dis*. 2012;28:49-69.
45. Stancu IC, Vasconcelos B, Terwel D, Dewachter I. Models of  $\beta$ -amyloid induced Tau-pathology: the long and "folded" road to understand the mechanism. *Mol Neurodegener*. 2014;9:51.
46. Bennett RE, DeVos SL, Dujardin S, et al. Enhanced tau aggregation in the presence of amyloid  $\beta$ . *Am J Pathol*. 2017;187:1601-1612.
47. Mintun MA, Lo AC, Duggan Evans C, et al. Donanemab slows progression of early symptomatic Alzheimer's disease in phase 2 proof of concept trial. Presentation at the Alzheimer's & Parkinson's Diseases (AD/PD™) International Conference; Virtual; March 9-14, 2021.
48. Han X, Jovicich J, Salat D, et al. Reliability of MRI-derived measurements of human cerebral cortical thickness: the effects of field strength, scanner upgrade and manufacturer. *NeuroImage*. 2006;32:180-194.
49. Fox NC, Black RS, Gilman S, et al. Effects of Abeta immunization (AN1792) on MRI measures of cerebral volume in Alzheimer disease. *Neurology*. 2005;64:1563-1572.
50. Novak G, Fox N, Clegg S, et al. Changes in brain volume with bapineuzumab in mild to moderate Alzheimer's disease. *J Alzheimers Dis*. 2016;49:1123-1134.
51. Cummings J. The role of biomarkers in Alzheimer's disease drug development. *Adv Exp Med Biol*. 2019;1118:29-61.
52. Schneider LS, Qiu Y, Thomas RG, et al. Impact of potential modifications to Alzheimer's disease clinical trials in response to disruption by COVID-19: a simulation study. *Alzheimers Res Ther*. 2021;13:201.

## SUPPORTING INFORMATION

Additional supporting information can be found online in the Supporting Information section at the end of this article.

**How to cite this article:** Mazer NA, Hofmann C, Lott D. et al., Development of a quantitative semi-mechanistic model of Alzheimer's disease based on the amyloid/tau/neurodegeneration framework (the Q-ATN model). *Alzheimer's Dement*. 2022;1-11. <https://doi.org/10.1002/alz.12877>